Proceedings of FDR2019
International Topical Workshop on Fukushima Decommissioning Research
May 24-26, 2019. J-Village, Naraha, Fukushima, Japan

FDR2019-1006

3D RECONSTRUCTION FOR UNDERWATER INVESTIGATION AT FUKUSHIMA DAIICHI NUCLEAR POWER STATION USING REFRACTIVE STRCTURE FROM MOTION

Xiaorui Qiao
The University of Tokyo
Tokyo, Japan

Atsushi Yamashita
The University of Tokyo
Tokyo, Japan

Hajime Asama
The University of Tokyo
Tokyo, Japan

Keywords: Underwater robots, 3D reconstruction, Structure from Motion, Refraction.

ABSTRACT

Three-dimensional (3D) reconstruction of the Primary Containment Vessel (PCV) internal structure provides useful information for cleanup of the fuel and debris submerged in the coolant. This internal structure can be recovered by Structure from Motion (SfM) technique using the investigation video sequences, such as the video captured by an underwater robot at Unit 3 PCV. However, the inside of Unit 3 PCV is filled with coolant. This underwater environment is different from the air environment. Thus, the camera equipped on the robot is confined in a waterproof camera housing. Light rays entering to the camera are refracted twice in this situation. One happens at the interface of water and camera housing, and the other happens at the interface of camera housing and the air. The refraction will result in geometric distortion in 3D reconstruction. In this paper, we propose a Refractive Structure from Motion (RSfM) approach to solve the refractive distortion problem during the 3D reconstruction. The approach includes camera system modeling, camera housing calibration, camera system pose estimation and geometric reconstruction. The camera system modeling method based on ray tracing is proposed to model the camera system of the underwater robot sent to Unit 3 PCV. A new camera housing calibration is based on back-projection error is proposed to achieve accurate modeling. Furthermore, camera system pose estimation based on modeled camera system is proposed for the geometric reconstruction. Finally, the 3D reconstruction can be obtained by triangulation. The effectiveness of proposed approach is confirmed using the video captured by the underwater robot at Unit 3 PCV of Fukushima Daiichi Nuclear Power Station. The geometric reconstruction results show that the proposed method can reduce the refractive distortion effectively and achieve better results than the conventional SfM method.

1. INTRODUCTION

The Fukushima Daiichi Nuclear Power Station has been facing crisis since 2011 Tohoku Earthquake and Tsunami (Ogawa, 2018, Masuda, 2018). One of the tasks is to remove the contaminated debris from the PCV. However, due to the highly radioactive environment and narrow penetration hole to access to the PCV, the internal status of PCV is almost unknown.

To give detail of investigation, several robots were developed for this highly radiated environment (Nagatani et al., 2011, Arai, 2018). An investigation carried out by Tokyo Electric Power Company (TECPO, 2015) on October 2015 found that the PCV of Unit 3 is filled with 6-meter-deep coolant. Fuel and other debris with radiation are submerged in the coolant. An extremely important task is to clean up the radiated debris in the plant. In this highly radiated environment, it is impossible for human to accomplish the task and the clean-up task may rely on the robotic techniques. Thus, the debris must be located and mapped in the 3D internal structures. The 3D reconstruction of the inside of PCV is essential to provide useful information for the cleanup and reduce the unknown factors for human and robots (Asama, 2018).

An underwater robot equipped with cameras and LED lights was sent to the Unit 3 PCV filled with coolant (Adachi, 2018). The robot captured the video in the PCV and collected information about the key structures. SfM using a single camera, as one of the 3D reconstruction techniques, can estimate the camera pose meanwhile reconstruct the 3D structure from the image sequences captured by the camera. Compared with hybrid or stereo camera systems (Bruno et al., 2011, Bastanlar et al., 2012), the rescue robots can be designed compactly using one single camera for narrow disaster area investigation.

SfM has been received intensive investigations (Aliakbarpour et al., 2015, Li et al., 2015). However, these studies are effective in air environment. In underwater environments, typically, the camera is confined in a waterproof housing. Thus, the light rays are refracted twice. One happens at the interface of water and the camera housing, and the other happens at the interface of the camera housing and the air. To obtain accurate 3D reconstruction, one challenge is the refraction during the image formation.

In this paper, we propose a SfM approach to solve the refraction problem. The approach solves the refraction

problem based on the camera system modeling, camera housing parameter estimation and camera system pose estimation.

The remainder of this paper is as below. Section 2 describes the proposed approach. Section 3 gives a brief description of the experiment and the result. Section 4 presents the conclusion.

2. APPROACH

Refraction is considered in camera system modeling, camera housing calibration and camera pose estimation in proposed approach.

2.1 Camera System Modeling

The robot camera system can be modeled based on the mechanical design as shown in Fig. 1. The shape of camera housing is cylindrical, and the camera is confined in the camera housing. When a light ray projects back to the outside from camera center, it can be segmented to three parts. $\mathbf{r}_a$ is the ray in the air, $\mathbf{r}_\mathrm{h}$ is the ray passing through the camera housing, and $\mathbf{r}_\mathrm{w}$ is the ray in the water. The refractive angles are θ_1 to θ_4. n_w, n_h, n_a are refractive index of water, camera housing and air, respectively. $\mathbf{N}_1$ and $\mathbf{N}_2$ are the normal on the refractive points, respectively.

According to the ray tracing and Snell law, the camera system can be modeled as below:

$$\tilde{\mathbf{r}}_\mathrm{h} = \frac{n_\mathrm{a}}{n_\mathrm{h}}\tilde{\mathbf{r}}_\mathrm{a} - \left(\frac{n_\mathrm{a}}{n_\mathrm{h}}\cos\theta_4 - \sqrt{1-\left(\frac{n_\mathrm{a}}{n_\mathrm{h}}\right)^2\sin^2\theta_4}\right)\tilde{\mathbf{N}}_2 \quad (1)$$

$$\tilde{\mathbf{r}}_\mathrm{w} = \frac{n_\mathrm{h}}{n_\mathrm{w}}\tilde{\mathbf{r}}_\mathrm{h} - \left(\frac{n_\mathrm{h}}{n_\mathrm{w}}\cos\theta_2 - \sqrt{1-\left(\frac{n_\mathrm{h}}{n_\mathrm{w}}\right)^2\sin^2\theta_2}\right)\tilde{\mathbf{N}}_1 \quad (2)$$

The ray and normal vectors with tilde in the above equations mean the normalized vectors. Therefore, the light ray from a pixel to a corresponding point can be traced if the relative pose of camera to the camera housing is known. In next subsection, the detail of how to determine the relative pose will be described.

2.2 Camera Housing Calibration

To determine the relative pose of the camera to the camera housing, we propose a novel but simple calibration method. In the calibration, the camera relative position and rotation to the camera housing will be determined. We estimate these parameters by minimizing the back-projection error.

As shown in Fig. 2, a calibrated camera is confined in a camera housing. The camera housing center is set at **H**, and the camera center is set at **C**. The relative rotation and translation of camera to the camera housing are $\mathbf{R}_\mathrm{CH}$ and $\mathbf{t}_\mathrm{CH}$, respectively. The world coordinate system origin is set on the checkerboard. Suppose $\mathbf{X}_n^W$ is a known point on the checkerboard, and the corresponding pixel is $\mathbf{x}_n$. **R** and **t** are the rotation and translation of world coordinate system relative to the local camera system, respectively. According to Eq. (1) and Eq. (2), the estimated point, $\hat{\mathbf{X}}_n^W$, can be represented by the unknown parameters need to estimate.

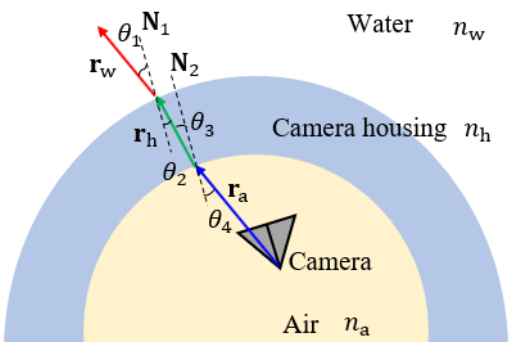

Fig. 1 The Camera System Modeling

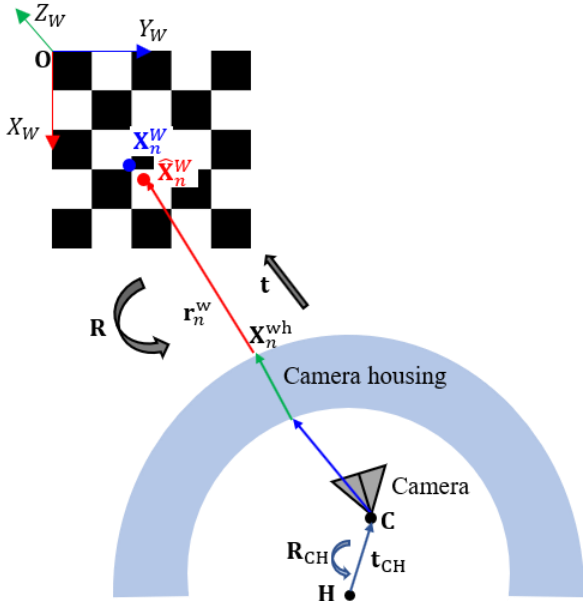

Fig. 2 Camera Housing Calibration

If we minimize the distance between the estimated point and the ground truth, the unknown parameters can be estimated during the optimization process. If *M* views are obtained, and each view contains *N* points, the total points for the calibration are *MN*. The cost function is the sum of the squared distance of all the corner points.

$$J = \sum_{m=1}^{M}\sum_{n=1}^{N}\left\|\hat{\mathbf{X}}_{mn}^W - \mathbf{X}_{mn}^W\right\| \quad (3)$$

This cost includes unknown rotation and translation need to estimate. During the optimization process, the relative pose of camera to the camera housing can be estimated.

2.3 Camera Pose Estimation

The relative pose between two local camera system can be estimated using modeled camera system in Subsection 2.1. As shown in Fig. 3, the robot has moved from location, L1, to location, L2. If the relative pose can be estimated, the point **X** can be reconstructed by triangulation. In this section, we propose a method to estimate the relative pose between two camera system based on the modeled camera system.

As depicted in Fig. 3, the rays from two camera system in different view intersect at point **X**. The rays can be represented by plücker line, which is an efficient way to represent lines in 3D space (Pless, 2003). Thus, the equation as below can be obtained.

$$\mathbf{L} = (\mathbf{d}, \mathbf{m}) = (\mathbf{r}_\mathrm{w},\ \mathbf{X}_\mathrm{hw} \times \mathbf{r}_\mathrm{w}) \quad (4)$$

where **d** and **m** are the direction and moment of the plücker line, respectively. $\mathbf{r}_\mathrm{w}$ is the vector in the water, and $\mathbf{X}_\mathrm{hw}$ is the intersecting point of the ray in the water at the camera

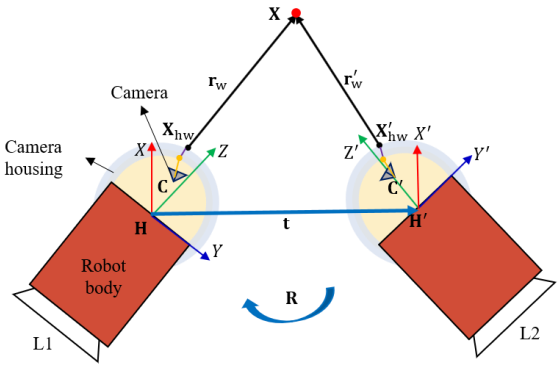

Fig. 3 Camera Pose Estimation

housing.

In the camera system at the second location, the ray in the water can be represented similarly as Eq. (4).

$$\mathbf{L}' = (\mathbf{d}', \mathbf{m}') = (\mathbf{r}'_w,\ \mathbf{X}'_{hw} \times \mathbf{r}'_w) \tag{5}$$

To estimate the relative camera pose of these two local camera systems, the plücker vectors of the ray in the second local camera system are transformed to the first local camera system by rotation **R** and translation **t**. According to property of the plücker line, the intersection of two lines can be described as below:

$$\mathbf{d}^\top \mathbf{m}'^W + \mathbf{m}^\top \mathbf{d}'^W = 0 \tag{6}$$

Thus, according to Eq. (4), Eq. (5) and Eq. (6), the equation as below can be obtained.

$$\begin{pmatrix} \mathbf{r}_w \\ \mathbf{m} \end{pmatrix}^T \begin{pmatrix} [\mathbf{t}]_\times \mathbf{R} & \mathbf{R} \\ \mathbf{R} & \mathbf{0} \end{pmatrix} \begin{pmatrix} \mathbf{r}'_w \\ \mathbf{m}' \end{pmatrix} = 0 \tag{7}$$

$[\mathbf{t}]_\times$ is the skew-symmetric matrix of **t**. If the corresponding points are obtained using feature detection and matching method, the related rays can be calculated based on Eq. (2). The unknown parameters in Eq. (7) are rotation, **R**, and translation, **t**. Thus, the relative pose **R** and **t** can be solved. A point can be reconstructed using triangulation method after the camera pose estimation.

3. EXPERIMENTS

The experiments include two parts: camera housing calibration to determine the related housing parameters and Unit 3 PCV internal scene reconstruction using the photos captured during the robot investigation.

3.1 Camera Housing Calibration

Several checkerboard patterns were captured using the camera system of the robot for the Unit 3 PCV internal investigation as shown in Fig. 4. According to the proposed calibration method in Subsection 2.2, the relative pose of the camera to the camera housing can be estimated. We use the average values of the estimated parameters as our camera modeling parameters as shown in Table 1. In Table 1, we convert the rotation matrix to Euler angles. α, β and γ are rotation angles related to *X*, *Y* and *Z* axis, respectively. t_x, t_y and t_z are translations of camera center to camera housing center in *X*, *Y* and *Z* direction.

Table 1 Estimated Parameters

Rotation angle	α	β	γ
Average (deg)	0.78	-0.66	-1.20
Translation	t_x	t_y	t_z
Average (mm)	0.61	1.39	35.08

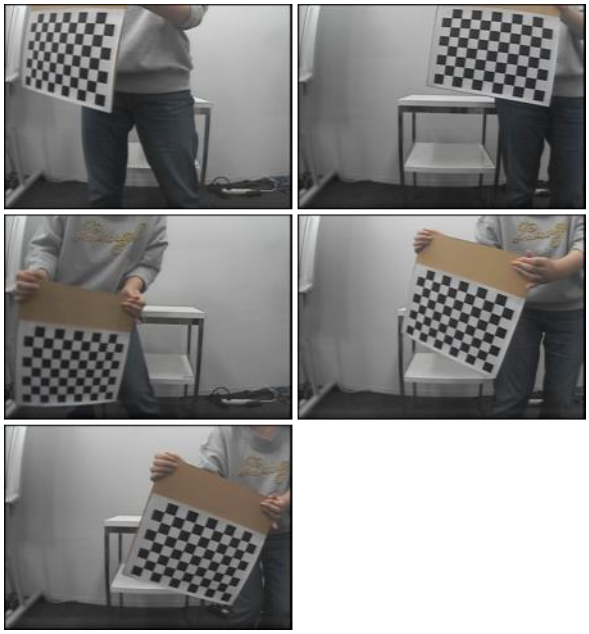

Fig. 4 Checkerboard patterns for Calibration

As depicted in Table 1, the camera has slight rotation to the camera housing and a major translation in *Z* direction. The results are also consistent with the design parameters. Thus, the proposed calibration method can estimate the related parameters precisely. After obtaining the camera housing parameters, the robot camera system can be modeled accurately using method in Subsection 2.1.

3.2 Unit 3 Scene Reconstruction

We use photos captured at inside of the Unit 3 PCV to reconstruct the 3D structures. In the experiment, we chose a typical scene as the input of the proposed approach. The images have been enhanced using our previous proposed enhancement method (Qiao et al., 2018) as shown in the right image of Fig. 5. The contrast and color of the image are improved.

We used two views of enhanced image to obtain the 3D reconstruction of this scene. The correspondences are computed using dense flow method (Tao et al., 2012). Thus, a dense reconstruction can be obtained as shown in the left image of Fig. 6. The structure is successfully reconstructed.

We also compared our proposed method with the conventional SfM method. As shown in the right image of Fig. 6, the recovered structure is distorted, especially the angle between two beams. However, the proposed method can recover the structure accurately compared with the conventional method. Conventional method is distorted because the refraction problem is not considered.

Fig. 5 Captured Images at Unit 3 PCV

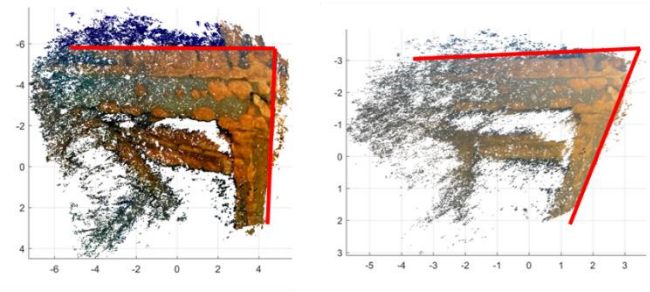

Fig. 6 Comparison of proposed method and conventional SfM

4. CONCLUSIONS

In this paper, we proposed an approach to reconstruct the structures inside of Unit 3 PCV by considering the refraction. To achieve accurate reconstruction, the camera system of the investigation robot was modeled based on ray tracing and Snell's law. We also proposed a simple but novel method to obtain the parameters between the camera and camera housing. Finally, the relative camera pose can be estimated based on the modeled camera system. The experiment results show that our method can reduce the distortion caused by refraction and achieve accurate 3D reconstruction compared with the conventional SfM method.

ACKNOWLEDGMENTS

The authors would like to thank IRID and TOSHIBA for supporting this research.

REFERENCES

Ogawa, T., 2018, Forefront of Nuclear Power Decommissioning -- Toward Fukushima Daiichi NPS Decommissioning -- Status and Issues for Technology Development, The Journal of The Institue of Electrical Engineers of Japan, Vol. 138, No.8, pp. 518-521.

Masuda, N., 2018, Fukushima Daiichi Decontamination and Decommissioning: Current Status and Challenges, Journal of The Robotics Society of Japan, Vol.36, No.6, pp. 384-388.

Nagatani, K., et al., 2011, Redesign of rescue mobile robot Quince, in Proceedings of the 2011 IEEE International Symposium on Safety, Security, and Rescue Robotics, pp. 13-18.

Arai, T., 2018, R&D on Robotics for Decommissioning of Fukushima Daiichi, Journal of The Robotics Society of Japan, Vol. 36, No. 6, pp. 389-394.

TECPO, 2015, Investigation Results of the Inside of Unit 3's Primary Containment Vessel (PCV). [Online] Available at: http://www.tepco.co.jp/en/nu/fukushima-np/handouts/2015/images/handouts_151020_01-e.pdf [Accessed 2 March 2019]

Asama, H., 2018, Utilization of Robot Technology in Decommissioning of Fukushima Daiichi Nuclear Power Station and Its Future Issues, Journal of The Robotics Society of Japan, Vol. 36, No. 6, pp. 380-383

Adachi, H., 2018, Investigation Robots for Inside Primary Containment Vessel of Fukushima Daiichi Nuclear Power Station, Journal of The Robotics Society of Japan, Vol. 36, No. 6, pp. 395-398.

Bruno, F., et al., 2011, Experimentation of structured light and stereo vision for underwater 3D reconstruction, ISPRS Journal of Photogrammetry and Remote Sensing, Vol. 66, No. 4, pp. 505-518.

Bastanlar, Y., et al., 2012, Multi-view structure-from-motion for hybrid camera scenarios, Image and Vision Computing, Vol. 30, No.8, pp. 557-572

Aliakbarpour, H., et al., 2015, Fast structure from motion for sequential and wide area motion imagery, In Proceedings of the 2015 IEEE International Conference on Computer Vision Workshops, pp. 34-41

Li, Z., et al., 2015, Simultaneous video defogging and stereo reconstruction, In Proceedings of the 2015 IEEE Conference on Computer Vision and Pattern Recognition, pp. 4988-4997.

Pless, R., 2003, Using many cameras as one, In Proceedings of the 2003 IEEE Computer Society Conference on Computer Vision and Pattern Recognition, pp. 587-589.

Qiao, X., et al., 2018, Visibility Enhancement for Underwater Robots Based on an Improved Underwater Light Model, Journal of Robotics and Mechatronics, Vol. 30, No. 5, pp. 781-790.

Tao, M., et al., 2012, SimpleFlow: A Non-iterative, Sublinear Optical Flow Algorithm, Computer Graphics Forum, Vol. 31, No. 2, pp. 345-353